

## High frequency measurements on an AlN/GaN-based intersubband detector at 1550 and 780 nm

D. Hofstetter,<sup>1,a)</sup> E. Baumann,<sup>1</sup> F. R. Giorgetta,<sup>1</sup> J. Dawlaty,<sup>2</sup> P. A. George,<sup>2</sup> F. Rana,<sup>2</sup> F. Guillot,<sup>3</sup> and E. Monroy<sup>3</sup>

<sup>1</sup>*Institute of Physics, University of Neuchatel, 1 A.-L. Breguet, CH-2000 Neuchatel, Switzerland*

<sup>2</sup>*Department of Electrical and Computer Engineering, Cornell University, Duffield Hall, Ithaca, New York 14853, USA*

<sup>3</sup>*CEA Grenoble, 17 Rue des Martyrs, 38054 Grenoble, France*

We report on high frequency measurements on an AlN/GaN-based intersubband detector using mode-locked solid state lasers. Our experiments involving laser wavelengths of 1550 and 780 nm demonstrate not only the capability of such devices to work both at the fundamental and at a higher order intersubband transition, but they also allowed us to push the high frequency detection limit up to a value of 13.3 GHz. From the shape of the harmonic decay, we conclude that this limit is not due to intrinsic properties of the detector.

Intersubband transitions in AlN/GaN-superlattices have experienced an intense period of research, which has resulted in the demonstration of several prototype devices such as intensity modulators, optically pumped light emitters, and photodetectors.<sup>1-3</sup> Since intersubband excitations in nitride semiconductor quantum wells have an extremely short lifetime on the order of 180–370 fs,<sup>4,5</sup> it is expected that further research in this direction will have a high practical pay off for future high speed telecommunication systems. More specifically, near-infrared photodetectors operating at long haul fiber telecom wavelengths and based on intersubband transitions in AlN/GaN-based superlattices have recently been demonstrated for frequencies approaching 3 GHz.<sup>6,7</sup> In order to push the maximum detection frequency toward the intrinsic limit, which is believed to lie in the multi-ten-gigahertz range, it is important to understand the current—mostly extrinsic—limitations of these devices in terms of impedance mismatch, parasitic capacitance, and inductance. On the other hand, a refined analysis of the intrinsic detection properties, especially at high frequencies, will allow us to further improve these devices. In this context, an important aspect concerns the detection of radiation whose photon energy is twice as large as the energy of the fundamental 1 → 2 intersubband transition. For this purpose, a reliable characterization method offering easy access to high frequencies as well as different photon energies is needed. In our earlier experiments, we used directly modulated semiconductor laser;<sup>6</sup> however, this method is sensitive to electrical crosstalk. An interesting alternative avoiding the crosstalk problem is the use of short pulse, mode-locked solid state lasers.<sup>8</sup> In this case, the detector measures the shape of the single pulse, which contains components at higher harmonics of the pulse repetition frequency. Consequently, if the resulting response is analyzed in the frequency domain, one can directly measure the frequency response of the detector. In the following article, we describe the architecture and some basic characterization of a mode-locked fiber laser emitting at 1.55  $\mu\text{m}$ , and its use as a measurement tool for an AlN/GaN-based infrared detector. In addition, we present results of the same

AlN/GaN-based detector's response to a commercially available mode-locked solid state laser at 780 nm.

The mode-locked fiber laser system used for these experiments is schematically represented in Fig. 1(a). It is based on a semiconductor laser pumped Yb-doped fiber laser/amplifier using nonlinear polarization rotation. The details of pulse generation at 1550 nm based on Raman soliton self frequency shift in a photonic crystal fiber are reported elsewhere.<sup>9</sup> The inset of Fig. 2 depicts a typical spectral tunability range of the pulse source, while Fig. 2 shows an autocorrelation trace of the output pulse near 1550 nm. A dielectric filter was used to spectrally isolate the generated pulses at 1550 nm from the rest of the emitted radiation. At 1550 nm, we measured typical average powers of 2 mW, a repetition rate of 30 MHz, and a pulse duration of <200 fs, corresponding to peak powers on the order of 0.3 kW. As will be shown below, an analysis of the output power as a function of polarization angle shows that the light is strongly

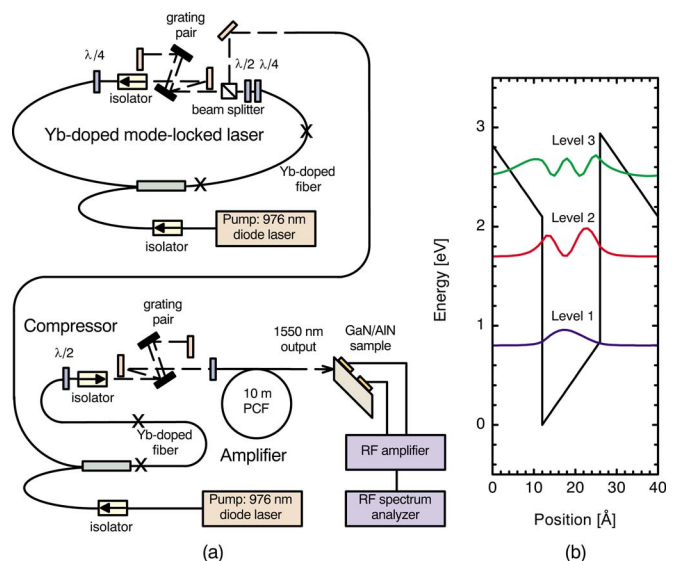


FIG. 1. (Color online) (a) Schematic representation of the mode-locked fiber laser and amplifier setup used in this work. (b) Simulation of the band structure with energy levels of the quantized states 1, 2, and 3 showing nearly equal spacing.

<sup>a)</sup>Electronic mail: daniel.hofstetter@unine.ch.

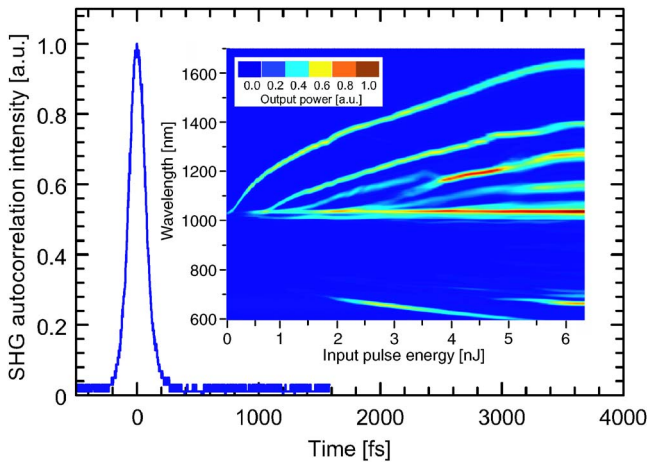


FIG. 2. (Color online) Autocorrelation trace of a laser pulse at 1550 nm showing a full width at half maximum of  $<200$  fs. The inset shows wavelength vs pump power curves of the laser output behind the Raman photonic crystal fiber wavelength shifter.

elliptically polarized. For those experiments involving 780 nm radiation, we used a commercial Ti-sapphire laser (Spectra Physics, Tsunami 3960-LLS) with a pulse repetition rate of 81 MHz, 1.5 W average power, 150 fs pulse width, and a peak power of 120 kW.

The intersubband detector investigated in this work consists of a 40 period superlattice with 1.5 nm thick Si-doped ( $5 \times 10^{19} \text{ cm}^{-3}$ ) GaN quantum wells and 1.5 nm thick undoped AlN barriers. A simulated conduction band structure along with the relevant wave functions of levels 1, 2, and 3 is shown in Fig. 1(b). The active region of this device is grown by molecular beam epitaxy on an AlN template and covered with a 100 nm thick AlN cap. The dark reference contact is connected to the ground, while the illuminated signal contact is wire bonded ( $L_{\text{bond}}=6.5$  mm) to the central pin of an sub-miniature version A (SMA) connector. The incoming light is focused to the signal contact via an antireflection coated lens ( $L_{\text{focus}}=50$  mm). Amplification of the detector's electrical signal is achieved via a low noise NexTec NBL00558 amplifier (1–12.5 GHz, 25 dB gain, 3 dB noise figure), and a broadband SHF 806P amplifier (40 kHz–32 GHz, 27 dB gain, 7 dB noise figure). Band structure simulations of this particular AlN/GaN-based detector structure have resulted in optical intersubband transition energies of  $E_{12}=807$  meV and  $E_{13}=1610$  meV, corresponding to detection wavelengths of  $\lambda_{12}=1540$  nm and  $\lambda_{13}=772$  nm. Interestingly,  $E_{12}$  seems to be almost exactly half of  $E_{13}$ , a prediction which will be confirmed by our measurements below.<sup>1</sup> Due to the strong internal fields and the concomitant asymmetry of the quantum wells, neither of these transitions is strictly forbidden; they can thus all be observed experimentally.

Since the optical signal consists of a train of pulses at either 30 or 81 MHz repetition rate, the resulting detector response is expected to be a train of electrical pulses with frequency components at the harmonics of either 30 or 81 MHz. To analyze these harmonics, the signal was sent to an HP8564E radio frequency (rf) spectrum analyzer. For alignment purposes, we chopped the optical beam at 2 kHz, and amplified the detector response with a Stanford Research Systems S560 current amplifier (current gain  $\approx 10^4$ ), which was connected to an oscilloscope. In order to measure the polarization sensitivity, a half wave plate was added to the beam. As expected for an intersubband device, the detector

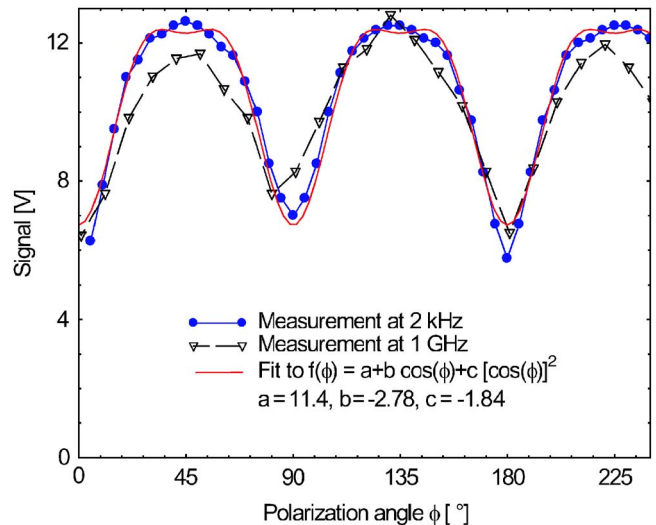


FIG. 3. (Color online) Optical response of the detector at 2 kHz and 1 GHz as a function of polarization angle  $\phi$ . The nonlinearity of the detector clearly distorts the expected cosine curve. The red line is a fit to the 2 kHz curve according to the function  $f(\phi)=a+b \cos(\phi)+c[\cos(\phi)]^2$ . The angles at integer multiples of  $90^\circ$  correspond to TE polarization, where the detector response is supposed to be weak.

showed a polarization ratio on the order of  $>15:1$  under illumination with a linearly polarized continuous diode laser beam at 1550 nm.

Figure 3 shows the dependence of the detector response on the polarization angle of the incident light under illumination with the 1550 nm mode-locked fiber laser. The detector shows a polarization dependent response both at low frequency ( $\sim 2$  kHz) as measured by the oscilloscope, and at high frequencies (34th harmonic of the pulse repetition rate  $\sim 1$  GHz) as measured by the rf spectrum analyzer. Instead of the expected cosine function, a distorted periodic function is observed; in addition, there is a large offset which is due to the elliptical polarization of the fiber laser beam. Based on the fact that the detector shows a quadratic deviation from linearity as outlined in Ref. 6, we performed a fit using the function  $f(\phi)=a+b \cos(\phi)+c[\cos(\phi)]^2$ . Such a fit to the 2 kHz curve is shown as well in Fig. 3. The good agreement between the measured points and the fit confirms again that we have to take into account saturation effects, especially when illuminating at high peak powers on the order of hundreds of watts.

Turning now to high frequency testing of the detector using the decay rate of the harmonic peaks, we have to make sure that we mathematically understand the behavior of these peaks. For the sake of mathematical simplicity, we assume pure soliton pulses with a width which is characterized by their full width at half maximum  $a$  divided by 1.76.<sup>10</sup> Since in a mode-locked laser these pulses follow each other in regular intervals characterized by parameter  $b$ , we can write the entire pulse stream as a convolution between a comb of delta peaks,  $\Pi(x)$ , and the soliton function

$$f(t) = \frac{1/a}{\cosh^2(t\pi/a)} * \frac{1}{b} \Pi(t/b),$$

where  $*$  denotes a convolution. The Fourier transform of this function using the definitions of Bracewell<sup>11</sup> is the product of the Fourier transforms of the single functions

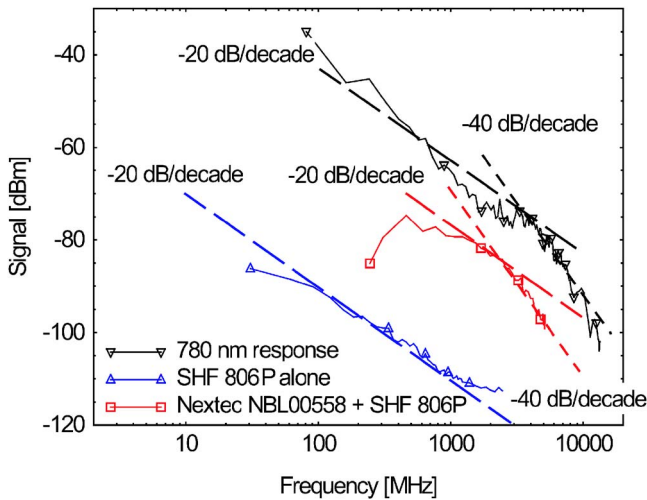


FIG. 4. (Color online) High-frequency response of the AlN/GaN-based detector as measured using the ultrashort pulses from the Raman shifted mode-locked fiber laser. The blue line was obtained with a broadband amplifier whereas the red line corresponds to a measurement using both low noise and broadband amplifier (both for 1550 nm radiation). The black curve corresponds to the response to the 780 nm radiation. Dashed lines are guides for the eye.

$$F(\omega) = \frac{2a\omega}{\sinh(a\omega\pi)} \Pi(b\omega).$$

In the above functions,  $t$  is the time and  $\omega$  the angular frequency. For our specific case,  $a=100$  fs and  $b=33$  ns; in addition, due to setup limitations our frequency measurements are not going beyond 15 GHz so that  $2a\omega/\sinh(a\omega\pi) \approx 2 = \text{constant}$  even for the highest experimental frequencies. On the other hand, the 3 dB frequency of  $F(\omega)$  is at 0.76 THz. Thus, if we would measure with an ideally fast photodetector and remain below roughly 15 GHz, we should see a regular series of nondecaying delta peaks spaced by  $1/b=30$  MHz in the frequency domain. However, if we actually observe a decay of these peaks, then this must be entirely due to the limited speed of the detector, at least for all frequencies which are sufficiently far from 0.76 THz.

Figure 4 shows the frequency characteristics that we have actually measured with the AlN/GaN-based intersubband detector. Each point corresponds to the height of a harmonic peak at that particular frequency. In the lower blue curve, we present the resulting response from a measurement amplified with a broadband amplifier SHF 806P only, which led to a maximal measurement frequency at 2 GHz. There is a nearly constant slope of  $-20$  dB/decade up to about 2.3 GHz. The smaller slope at low frequencies is due to the detector's low-pass corner frequency of roughly 35 MHz, in agreement with our earlier measurements.<sup>6</sup> In the upper red curve, we used both the low-noise and the broadband amplifier; therefore, the maximally measurable frequency could be pushed up to 5 GHz. For frequencies lower than about 1 GHz, the low frequency cutoff of the amplifier is well visible. Otherwise, the slope is constant at  $-20$  dB/decade. At a frequency of 2.3 GHz, the slope suddenly becomes twice as steep, namely  $-40$  dB/decade. This observation agrees to the one reported earlier and was at that time attributed to the 3 dB frequency of one of the amplifiers. Since in the present experiment no amplifier reached its frequency limit, this slope change must be either due to intrinsic detec-

tor properties or parasitics in the mounting. Since the measured frequency behavior can be modeled by two serial low-pass filter characteristics, one of them is attributed to the parasitic inductance of the 6.5 mm long bond wire,<sup>12</sup> while the other one must be due to the parasitic capacitance between the two contacts. Let us turn finally to the black curve which shows the detector's frequency response at the wavelength of the mode locked solid state laser (780 nm). Apart from the fact that we were able to measure a response up to a remarkably high frequency of 13.3 GHz (165th harmonic), this measurement shows also a slightly different frequency behavior. Instead of 2.3 GHz as seen at 1550 nm, the slope change from  $-20$  to  $-40$  dB/decade occurs at roughly 3 GHz. However, even assuming a very weak absorption from the  $1 \rightarrow 3$  intersubband transition when compared to the  $1 \rightarrow 2$  transition, a 1.5 W laser beam at 780 nm will lead to considerably severe device heating than the 2 mW beam at 1550 nm. The observed difference can therefore be explained easily by a higher device temperature which reduces the device resistance and thus the time constant of one of the low-pass filters.

In conclusion, we have presented high frequency measurements for AlN/GaN-based intersubband detectors. The measurement method is based on optical generation of the measurement frequency using mode-locked solid state lasers. It has been shown that the presented AlN/GaN-based device worked up to 13.3 GHz with a frequency behavior determined by parasitic effects such as the inductance of the bond wire. Our experiments confirmed also in an unambiguous way earlier band structure calculations in 1.5 nm GaN quantum wells, which predicted a  $1 \rightarrow 3$  intersubband transition at nearly twice the energy of the  $1 \rightarrow 2$  transition. This is extremely valuable input for future device optimization.

The authors would like to acknowledge the US Office of Naval research under Grant No. N00014-08-1-4005 monitored by Dr. David Marquis, and the Professorship Program of the Swiss National Science Foundation for their generous financial support. Valuable discussions with Faisal R. Ahmad and Lester F. Eastman, both with Cornell University, are also gratefully acknowledged.

- <sup>1</sup>L. Nevou, M. Tchernycheva, F. H. Julien, F. Guillot, and E. Monroy, *Appl. Phys. Lett.* **90**, 121106 (2007).
- <sup>2</sup>A. Lupu, F. Julien, S. Golka, G. Pozzovivo, G. Strasser, E. Baumann, F. R. Giorgetta, D. Hofstetter, S. Nicolay, M. Mosca, and N. Grandjean, *IEEE Photonics Technol. Lett.* **20**, 102 (2008).
- <sup>3</sup>D. Hofstetter, E. Baumann, F. R. Giorgetta, M. Graf, M. Maier, F. Guillot, E. Bellet-Amalric, and E. Monroy, *Appl. Phys. Lett.* **88**, 121112 (2006).
- <sup>4</sup>J. D. Heber, C. Gmachl, H. M. Ng, and A. Y. Cho, *Appl. Phys. Lett.* **81**, 1237 (2002).
- <sup>5</sup>Z. Wang, K. Reimann, M. Woerner, T. Elsaesser, D. Hofstetter, E. Baumann, F. R. Giorgetta, H. Wu, W. J. Schaff, and L. F. Eastman, *Appl. Phys. Lett.* **89**, 151103 (2006).
- <sup>6</sup>D. Hofstetter, E. Baumann, F. R. Giorgetta, F. Guillot, S. Leconte, and E. Monroy, *Appl. Phys. Lett.* **91**, 131115 (2007).
- <sup>7</sup>D. Hofstetter, S.-S. Schäd, H. Wu, W. J. Schaff, and L. F. Eastman, *Appl. Phys. Lett.* **83**, 572 (2003).
- <sup>8</sup>A. Chong, W. H. Renninger, and F. W. Wise, *Opt. Lett.* **32**, 2408 (2007).
- <sup>9</sup>J. Dawlaty, A. Chong, and F. Rana, LEOS Summer Topical Meetings, Digest of the IEEE, 2007 (unpublished), Vol. 23, p. 157.
- <sup>10</sup>R. Paschotta, Encyclopaedia on Laser Physics and Technology ([http://www.rp-photonics.com/quasi\\_soliton\\_pulses.html](http://www.rp-photonics.com/quasi_soliton_pulses.html)).
- <sup>11</sup>R. N. Bracewell, *The Fourier Transform and its Applications*, 2nd ed. (McGraw-Hill, New York, 1986), p. 267.
- <sup>12</sup>D. Hofstetter, M. Graf, T. Aellen, J. Faist, L. Hvozdar, and S. Blaser, *Appl. Phys. Lett.* **89**, 061119 (2006).